Conformation and Environment of Channel-Forming Peptides: A Simulation Study

Jennifer M. Johnston,* Gabriel A. Cook,† John M. Tomich,† and Mark S. P. Sansom*
*Department of Biochemistry, University of Oxford, Oxford, United Kingdom OX1 3QU; and †Department of Biochemistry, Kansas State University, Manhattan, Kansas 66506

ABSTRACT Ion channel-forming peptides enable us to study the conformational dynamics of a transmembrane helix as a function of sequence and environment. Molecular dynamics simulations are used to study the conformation and dynamics of three 22-residue peptides derived from the second transmembrane domain of the glycine receptor (NK_4-M2GlyR-p22). Simulations are performed on the peptide in four different environments: trifluoroethanol/water; SDS micelles; DPC micelles; and a DMPC bilayer. A hierarchy of α-helix stabilization between the different environments is observed such that TFE/water $<$ micelles $<$ bilayers. Local clustering of trifluoroethanol molecules around the peptide appears to help stabilize an α-helical conformation. Single (S22W) and double (S22W,T19R) substitutions at the C-terminus of NK_4-M2GlyR-p22 help to stabilize a helical conformation in the micelle and bilayer environments. This correlates with the ability of the W22 and R19 side chains to form H-bonds with the headgroups of lipid or detergent molecules. This study provides a first atomic resolution comparison of the structure and dynamics of NK_4-M2GlyR-p22 peptides in membrane and membrane-mimetic environments, paralleling NMR and functional studies of these peptides.

INTRODUCTION

Membrane proteins are estimated to account for ~30% of open reading frames (1) and constitute up to 50% of current drug targets (2). However, the number of high resolution structures that are known for membrane proteins, while growing exponentially (3), remains relatively small (http://blanco.biomol.uci.edu/membrane_proteins_xtal.html). The majority of membrane proteins are made up of bundles of transmembrane (TM) α-helices. TM helices appear to be intrinsically stable in membranes and membrane-like environments (4). Structures of isolated TM helices have been determined by NMR in nonaqueous solvents (5), in detergent micelles (6), and in lipid bilayers (7). The two-state folding model (8) and its more recent variants (9) are predicated upon TM helices as autonomous folding domains (10). It is therefore of interest to understand the intrinsic stability of TM α-helices as a function of environment, both from a structural biology (i.e., membrane protein folding), and from a chemical biology (e.g., TM α-helix (re)design (11,12)) perspective.

A number of TM α-helix peptides are able to form channels or pores in lipid bilayers. These include antibiotic and toxin-derived peptides(13,14), TM helices from viral ion channels (viroporins) (15), de novo designed peptides (16), and also peptide fragments derived from more complex ion channels. For example, the M2δ peptide corresponding to the pore-lining M2 helix of the nicotinic acetylcholine receptor has been studied in some detail in terms of function (17,18), structure (19), and simulation (20,21). These studies have provided much information on the nature of pore formation by α-helical bundles. However, a deeper understanding of the molecular origins of conformational stability of TM helix peptides is still required.

The glycine receptor (GlyR) is a chloride conducting, receptor-gated channel, mediating rapid inhibitory neurotransmission in the mammalian central nervous system. It is a member of the same family of ''Cys-loop'' receptor channels (22) as the nicotinic acetylcholine receptor and shares significant sequence homology, thus, may be presumed to share the same overall architecture. An NMR structure of a fragment of the GlyR corresponding to TM domains M2 and M3 (23) in solution in trifluoroethanol (TFE) revealed a conformation similar to that of the corresponding region in the nicotinic receptor, with both M2 and M3 being largely α-helical (24). A synthetic peptide corresponding to the sequence of the GlyR M2 segment has been shown to form anion conducting channels and to share a number of properties with the parent channel (25). Subsequently, a family of M2GlyR channel-forming peptides is being studied in detail both in terms of function and of structure (26). From a chemical biology perspective it is envisaged that manipulation of the M2GlyR sequence can minimize peptide aggregation in solution while increasing water solubility and self-assembly to form high-flux anion-conducting channels in a lipid bilayer. Such peptides would be of interest as a potential ion channel replacement therapy for chloride channelopathies (e.g., cystic fibrosis) (27).

Molecular dynamics (MD) and related simulations are of increasing importance in providing atomic resolution detail for the interactions of peptides and proteins with membrane

Submitted June 28, 2005, and accepted for publication September 26, 2005.

Address reprint requests to Mark S. P. Sansom, Tel.: 44-1865-275371; Fax: 44-1865-275273; E-mail: mark.sansom@bioch.ox.ac.uk.

Gabriel A. Cook's present address is Dept. of Chemistry and Biochemistry, University of California, San Diego, 9500 Gilman Dr., MC 0307 La Jolla, CA 92093.

0006-3495/06/03/1855/10 $2.00

doi: 10.1529/biophysj.105.069625

(28–30) and membrane-like (31–33) environments. A number of studies have used such simulations to explore in more detail the nature of pore-lining M2 peptides from the nicotinic acetylcholine receptor and related channels (21,34–36). In this article we employ MD simulations to explore the conformational dynamics of three M2GlyR peptides. In particular, we investigate the stability of the α-helical conformation as a function of environment. We have chosen three environments that reflect experimental studies of these and other TM peptides: i), a complex ''helix-promoting'' solvent system, namely trifluoroethanol and water (37); ii), detergent micelles (both SDS and DPC (38)); and iii), phospholipid (DMPC) bilayers (39). The results reveal a complex interplay between environment and sequence in governing the conformational stability of a TM helix.

METHODS

Peptides

Three M2GlyR peptides have been investigated. In each of these, four lysine residues have been added to the N-terminus of a fully active 22-residue truncated M2 sequence (KKKKPARVGLGITTVLTMTTQS; Fig. 1 *A*) (40). Note that although the sequence is truncated and four lysines are added to the N-terminus, for simplicity we refer to this peptide as NK_4-M2GlyR p22 WT (referred to as WT from now on). The structure of the truncated WT peptide have been determined by NMR in 40% TFE and shown to be substantially α-helical (26). A modified peptide, NK_4-M2GlyR p22 S22W (referred to as S22W from now on), has a single Trp substitution at the C-terminus, which reduces peptide aggregation and increases channel formation at reduced concentration. The NMR structure of this peptide in TFE/water suggests a more distorted conformation, with α-helix restricted to a 15-residue TM segment. A further substitution, yielding the peptide NK_4-M2GlyR p22 T19R,S22W (referred to as T19R,S22W from now on) has been shown to further promote chloride ion transport properties (see article by Shank et al. in this issue).

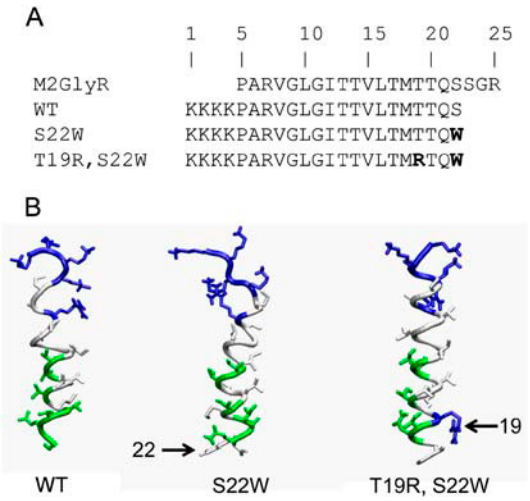

FIGURE 1 (*A*) Sequences of the three peptides, along with that of the M2 helix in the GlyR from which the peptides are derived. (*B*) Initial structures for the three peptides: WT, S22W, and T19R,S22W. The residues are colored according to their type: white = hydrophobic, green = polar, uncharged, and blue = polar, charged.

The starting structures for the simulations (Fig. 1 *B*) are taken from the NMR solution structures (in TFE/water) for the WT and S22W peptides. In each case, the structure used was the lowest energy conformer after minimization from a cluster of structures with the lowest NMR target function values. For T19R,S22W the NMR structure of which has not been determined in TFE/water an α-helical model was constructed by a simulated annealing based modeling procedure (41,42). For comparative simulations (see below) an α-helical model of WT was also generated by simulated annealing.

Simulation methods

Simulations were performed using GROMACS v3 (43) (www.gromacs.org). The ffgmx43a1 force field was used, modified for use with lipids, along with the SPC water model (44,45). During equilibration periods (see below) the temperature was controlled using the Berendsen thermostat (46) with a coupling constant $\tau_T = 0.1$ ps, and the pressure was controlled using the Berendsen barostat with a coupling constant of $\tau_P = 1$ ps. For the duration of the equilibration period, harmonic position restraints were applied to the heavy atoms of the peptide, with a force constant of 1000 kJ mol^{-1} nm^{-2}. During the 20-ns production runs, the temperature coupling was switched to the Nosé-Hoover method (47,48) with coupling constant $\tau_T = 0.5$ ps, and the pressure coupling was switched to the Parrinello-Rahman method (49) with a coupling constant of $\tau_P = 5$ ps. Periodic boundary conditions were employed, and long-range electrostatic interactions were treated using particle mesh Ewald (PME) summation (50). The LINCS algorithm (51) was used to constrain bond lengths. The simulation time step was 2 fs and coordinates were saved for analysis every 5 ps.

Simulations and their setup

Simulations were performed in four different environments: TFE/water, SDS micelles, DPC micelles, and DMPC bilayers (Table 1). Parameters for a 30% TFE/water system were from Fioroni et al. (52) because these had been used previously in simulations of peptides in this environment (37,53). Each peptide (i.e., WT, S22W, and T19R,S22W) was solvated using a preequilibrated box containing a 1:2 ratio of TFE molecules and water molecules, to which Cl^- ions were added to neutralize the system. After a 1-ns equilibration period, during which the heavy atoms of the peptide were

TABLE 1 Summary of simulations

Peptide*	Environment	Equilibration/ production duration (ns)	Temperature (K)	Cα RMSD† (nm)
WT (NMR structure)	DMPC	0.2 / 20	310	0.28
	DPC	0.5 / 20	300	0.48
	SDS	1.0 / 20	300	0.50
	30% TFE	1.0 / 20	300	0.79
WT (Model structure)	30% TFE	1.0 / 20	300	0.68
S22W (NMR structure)	DMPC	0.2 / 20	310	0.33
	DPC	0.5 / 20	300	0.22
	SDS	1.0 / 20	300	0.31
	30% TFE	1.0 / 20	300	0.75
T19R,S22W (Model structure)	DMPC	0.2 / 20	310	0.20
	DPC	0.5 / 20	300	0.24
	SDS	1.0 / 20	300	0.20
	30% TFE	1.0 / 20	300	0.49

*The sequences of the peptides are given in Fig. 1. System sizes ranged from ~18,000 to ~36,000 atoms.

†The root mean square deviation (RMSD) from the initial Cα atom coordinates, averaged over the last 10 ns of each simulation, is given.

positionally restrained, the peptide was simulated for a 20 ns production period. The parameters for dodecyl sulfate were derived using PRODRG website (54) (http://davapc1.bioch.dundee.ac.uk/programs/prodrg/). A toroidal geometry micelle of 60 SDS monomers was generated as described in Bond and Sansom (31). This was then solvated and the micelle was neutralized with 60 Na^+ ions, after which further ions were added to give an overall concentration of ~0.1 mM. This was subjected to a 1-ns equilibration period before the 20 ns production run. DPC parameters were as in Bond and Sansom (31). The micelle contained 55 detergent molecules. Counterions sufficient to neutralize the peptide were added to the system. Before the production run, a 0.5 ns equilibration was performed. For the lipid bilayer simulations, each peptide was inserted into a preequilibrated bilayer of 128 DMPC molecules, using a cavity formed by the removal of two or three DMPC molecules according to the shape of the peptide solvent accessible surface (as described previously (55)). This system was solvated and NaCl ions were added to give a concentration of ~0.1 mM. After the peptide insertion procedure, a further short equilibration simulation (0.2 ns) was performed before the production run.

Analysis and display

Simulations were analyzed using Gromacs routines and local code. Secondary structure analysis used DSSP (56). The integrity of the models generated was assessed using Procheck (57). Simulations were visualized using VMD (58) and images generated using Povray (http://www.povray.org/) and RasTop (http://www.geneinfinity.org/rastop/) (59).

RESULTS

Simulations and conformational drift

Each peptide (WT, S22W, and T19R,S22W) was simulated in four different environments (Table 1). In every case the environment is anisotropic. In TFE/water the TFE molecules form small clusters (52) that therefore provide the peptide with a locally anisotropic environment (Fig. 2 *A*). In the micelles, the polar headgroups are at the surface of the micelle, whereas the interior is formed by the hydrophobic chains (Fig. 2, *B* and *C*). Finally, in DMPC the peptide spans the lipid bilayer (Fig. 2 *D*).

A simple measure of the conformational stability of a peptide in a given environment is provided by the root mean square deviation (RMSD) from the initial conformation of the Cα atoms (Fig. 3). If we compare the RMSD versus environment for each peptide we see the following trends: for the WT peptide, TFE > SDS ≈ DPC > DMPC; for S22W, TFE > SDS ≈ DMPC > DPC; and for T19R,S22W, TFE > SDS ≈ DPC ≈ DMPC. Thus for all three peptides, the greatest degree of conformational drift is seen in TFE/water. All three peptides show comparable stability in the detergent micelle and lipid bilayer environments, with the drift being slightly lower in the bilayer environment in two out of three cases. If we compare the peptides in the micelles it seems that S22W and T19R,S22W are more stable than the WT peptide. The T19R,S22W peptide appears to be the most stable in the bilayer environment (although this may be due to starting from an α-helical model; this is addressed further below).

We have also compared the magnitude of the fluctuations in structure, by calculating the mean square fluctuations of Cα atoms (data not shown). For the WT peptide, the fluctuations are generally higher than for the other two peptides, especially in the SDS micelle environment where the WT fluctuations are an order of magnitude higher than those of S22W and T19R,S22W. For S22W and T19R,S22W only the TFE environment exhibited large fluctuations. Thus, this analysis parallels the picture provided by simple comparison of RMSDs.

Secondary structure

A more detailed comparison of the simulations was provided via examination of the secondary structures of the peptides as a function of time (Fig. 4 *A*). The WT peptide had the lowest initial α-helical content of all three peptides. However, the C-terminal α-helical regions remained quite well defined and throughout the simulations, especially in the bilayer (and SDS micelle, data not shown) environments. This correlates with the NMR structure of the WT peptide in TFE/water, which shows a well-defined C-terminal α-helix in all members of the ensemble in contrast to conformational heterogeneity in the N-terminal half of the peptide. In the DMPC bilayer simulation, there was an increase in the extent of the α-helix midway through the simulation, so that it extended from residues ~10–21. This amounts to ~45% of the peptide, i.e., an increase in α-helicity relative to the initial NMR derived structure (in TFE/water). Thus the bilayer environment promoted an α-helical conformation. The secondary

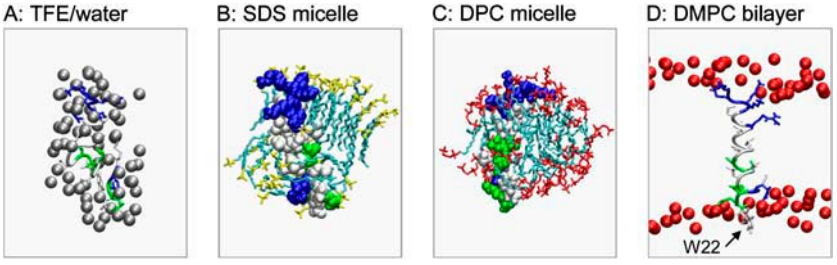

FIGURE 2 Snapshots of T19R,S22W in the four different environments. (*A*) 30% TFE/water mixture, with the peptide helix shown in as a ''tube'' colored as in Fig. 1 and van der Waals spheres for the carbon atoms of the CF_3 groups of those TFE molecules within a 5 Å cutoff of the peptide. (*B*) SDS micelle, with the peptide as van der Waals spheres and the detergent (*cyan*/*yellow*) in ''bonds'' format. (*C*) DPC micelle, with the peptide as van der Waals spheres and the detergent (*cyan*/*red*) in ''bonds'' format. (*D*) DMPC bilayer, with the peptide helix shown in as a ''tube'' and the phosphorus atoms of DMPC molecules (*red*) represented as van der Waals spheres.

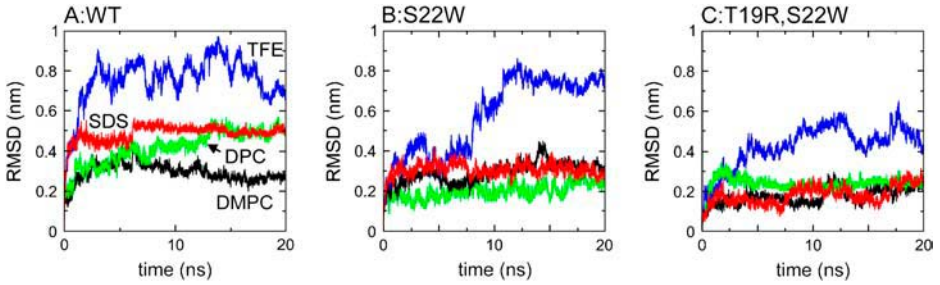

FIGURE 3 Conformational drift shown as Cα atom root mean square deviation (*RMSD*) from the starting structure for the simulations of the: (*A*) WT; (*B*) S22W; and (*C*) T19R,S22W peptides. In each case the RMSDs are shown for simulations in: TFE/water (*blue*); SDS micelles (*red*); DPC micelles (*green*); and DMPC bilayers (*black*).

structure in the SDS micelle and the TFE/water mixture were similar. In the SDS micelle the α-helical portion of the peptide (residues 13–20) remained constant for the duration of the simulation, with the remainder of the peptide adopting a random coil conformation, with a small amount of reversible bend/turn formation. The secondary structure in TFE was more time-variable, but residues 13–20 were again predominantly α-helical. The DPC micelle was intermediate between TFE or SDS and the bilayer, and once more, the C-terminal region remained α-helical.

The initial structure for S22W had a greater α-helical content than that for the WT peptide, with the α-helical portion encompassing residues 5–20, amounting to $\sim$70% of the peptide. This α-helix was stable throughout the final 18 ns of both the DPC micelle and the DMPC bilayer simulations. In DPC there was a recurrent transient break in the α-helix at residue I12. In the SDS micelle, the stable α-helical conformation was only retained by residues 5–16 whereas the four N-terminal Lys residues remained unstructured throughout. The secondary structure of this peptide in TFE/water was more complicated, with the initially α-helical portion exhibiting a fluctuating combination of conformations throughout the simulation.

The T19R,S22W peptide exhibited the highest α-helical content of the three peptides in the micellar and bilayer environment. In TFE/water the initial α-helix underwent a degree of dynamic unfolding over the duration of the simulation. During the first 2 ns of the simulation the α-helix loosened to adopt a π-helix conformation and for the duration of the simulation the peptide remained flexible and suffered reversible kinks and bends along the length of the peptide. In DMPC, α-helicity was maintained between residues 3 and 20 for nearly all of the simulation, although a transient distortion around residue 12 and some loss of helicity at the C-terminus showed that nonhelical conformations can be accessed.

To more fully illustrate the nature of the conformational changes undergone by the peptides, in Fig. 4, *B–E*, we show superimposed snapshots (saved every 2 ns) of the WT peptide as a function of environment. In each case it can be seen that the C-terminal α-helix is, to a greater or lesser extent, retained, whereas the N-terminal half of the molecule undergoes considerable conformational fluctuations. These fluctuations are clearly ranked as TFE/water $>$ micelle $>$ bilayer. Thus, even though the N-terminal half of WT is not α-helical when in a lipid bilayer, it seems to adopt a defined conformation and to undergo relatively small changes in conformation.

Interaction of peptides with environment: TFE/water

Having examined the conformational dynamics of the peptides as a function of environment, it is of interest to characterize the nature of the interactions of the peptides with their environments. The micro-heterogeneity of TFE/water around the peptides can be visualized by contouring the local TFE density so as to reveal TFE clusters around the surface of the peptide (Fig. 5). Thus, to some extent the local anisotropy of solvent may mimic a membrane environment. In particular, the charged and polar residues of the peptides appear to face regions of lower TFE density whereas the hydrophobic residues face higher density regions. We also note that the T19R,S22W peptide has a more continuous high local TFE density at its surface than the other two peptides. It is interesting to note that this high-density coating appears to correspond with the regions of the peptide that maintain their secondary structure, at least for the S22W and T19R,S22W peptides.

Interaction of peptides with environment: detergents and lipids

For the micelle and bilayer simulations, given the amphipathic nature of the detergent and lipid molecules, it is informative to quantify the numbers of molecules whose polar headgroups or hydrophobic tails are in contact with (defined using a 0.35-nm cutoff) the peptide as a function of time. In Fig. 6, we compare this for the T19R,S22W peptide as this was conformationally stable in the three environments (SDS, DPC, and DMPC). Comparing the two micelles, it is interesting that fewer interactions are provided by SDS than by DPC. This may reflect the smaller headgroup in the SDS molecule, and the less ''fluid'' environment provided by this detergent. Comparing DMPC and DPC, we see that in both simulations there are a substantial number of headgroup interactions with the peptide. With respect to the hydrophobic tails it appears that there are more contacts made in the micelle than in the bilayer.

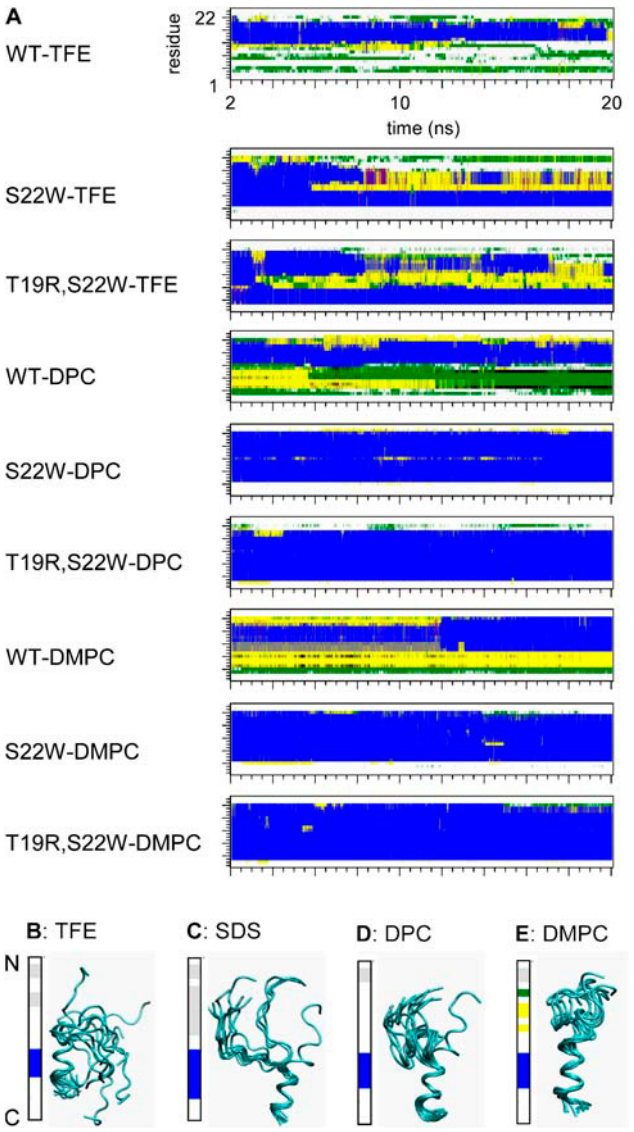

FIGURE 4 (*A*) Secondary structure (calculated using DSSP (53)) as a function of time for all three peptides in TFE/water, in DPC micelles, and in DMPC bilayers. Blue = α-helix; yellow = turn; purple = π-helix; light gray = coil; green = bend. (*C–E*) Snapshots (every 2 ns) of the WT peptide in the four different environments, fitted to the α-helical portion of the peptide. Alongside each peptide is a representation of the predominant secondary structure in that simulation. Defined structure is only recorded if it is prevalent for 90% of the simulation time. The secondary structure is calculated according to DSSP and the colors are as previously defined. White indicates that there is no single secondary structure that prevails for 90% of the simulation.

Given the importance of the headgroup interactions, and also the underlying design of the peptides, it is of interest to examine the nature of H-bonding interactions involving the C-terminal tryptophan residue in the DMPC bilayer simulations. Tryptophan residues play a key role in stabilizing membrane proteins within lipid bilayers (60–62). If we compare S22W and T19R,S22W (Fig. 7, *A* and *B*), we see that in both cases the Trp side chain, which is situated in the

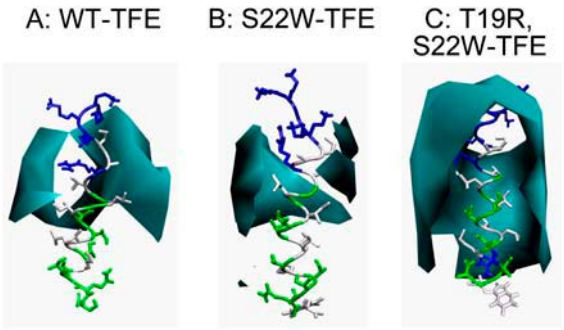

FIGURE 5 Clustering of TFE molecules around the three peptides. Snapshots of initial conformations of peptides superimposed on average TFE density contoured at 6 molecules nm^{-3}.

membrane/water interfacial region, can form H-bonds to both water molecules and to lipid headgroups. Indeed, in both cases there appears to be a slow (~10 ns) switching of the Trp between water and headgroup interactions.

We have also examined the importance of basic residues in interactions in the interfacial regions. Thus, in Fig. 7 *C*, we show H-bonds formed by the two arginine side chains of T19R,S22W (at positions 7 and 19). Again, interactions with both lipid headgroups and with water molecules are seen,

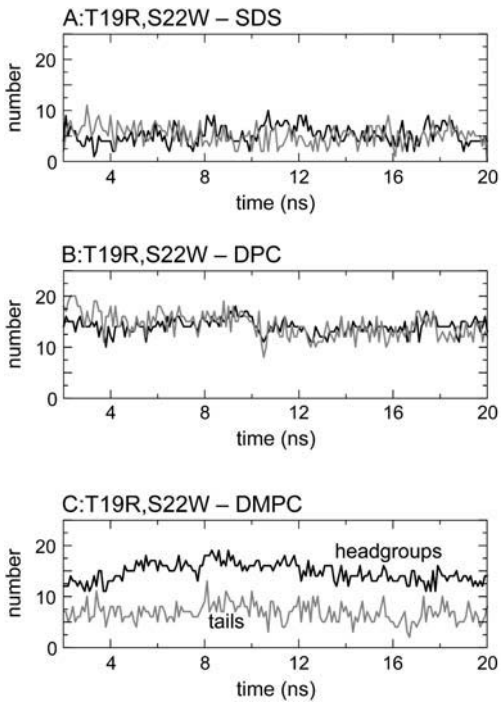

FIGURE 6 Detergent/lipid-peptide interactions for T19R,S22W. For each simulation the overall numbers of lipid-peptide interactions (defined using a cutoff of 0.35 nm) are shown as the numbers of lipid molecules making contact with a peptide atom. Black lines are for peptide interactions with detergent/lipid headgroups; gray lines are for interactions with detergent/lipid tails.

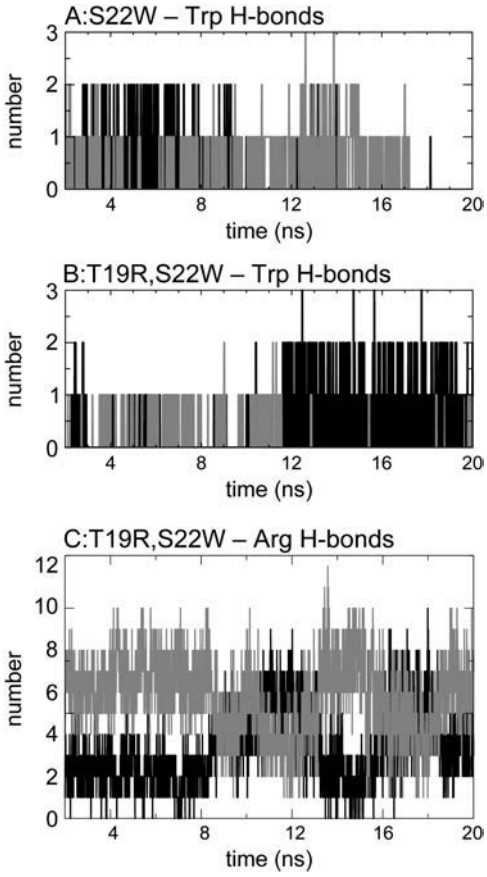

FIGURE 7 H-bond formation as a function of time showing interactions of Trp or Arg side chains with water molecules (*black lines*) and with lipid headgroups (*gray lines*) for: (*A*) Trp side chain of S22W in simulation S22W-DMPC; (*B*) Trp side chain of T19R,S22W in simulation T19R-DMPC; and (*C*) Arg side chains of T19R,S22W in simulation T19R-DMPC.

fluctuating on an ~5-ns timescale. In general, the N-terminal lysine residues form more H-bonds with the headgroups of the lipids and detergents than the C-terminal residues. However, there does seem to be a consistent pattern of H-bonding to the phosphate headgroups of DPC for the peptides with the S22W terminal substitution. The WT peptide only forms transient C-terminal H-bonds with the DPC headgroups.

Examples of the interactions of basic residues in the interfacial regions are shown in Fig. 8. For S22W one can see close interactions between the sulphates of two SDS molecules and the side chains of two of the N-terminal lysines (K2 and K4; Fig. 8 *A*). For T19R,S22W a complex network of H-bonds with the headgroups of two DMPC molecules is observed (Fig. 8 *B*). Thus, the arginine side chain forms two H-bonds to the carbonyl oxygen of an acyl chain of one DMPC molecule, and a further H-bond to an interfacial water molecule, which is in turn H-bonded to the phosphate oxygen of another DMPC molecule. These H-bond networks in the interfacial region are typical of those seen in simulations of more complex membrane proteins in PC bilayers (63).

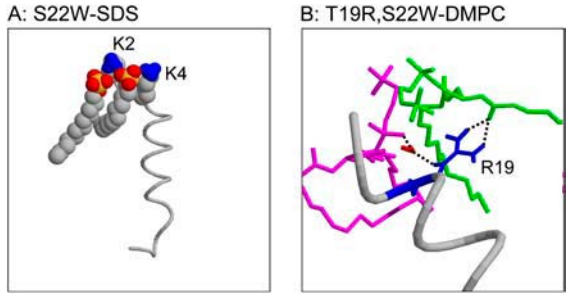

FIGURE 8 Snapshots of interactions between charged residue side chains and detergent or lipid headgroups. In panel *A*, the interactions between the sulphates of two SDS molecules and two N-terminal lysines (K2 and K4) of S22W are shown. In panel *B*, H-bonds of R19 (*blue*) of T19R,S22W and the headgroups of two DMPC molecules (*green*, *purple*) are shown. The side chain of R19 forms three H-bonds (indicated by *dashed black lines*): two to the carbonyl oxygen of an acyl chain of one DMPC (*green*), and one via a bridging water molecule (*red*) to the phosphate oxygen of another DMPC (*purple*) molecule.

DISCUSSION

Our results suggest a hierarchy of α-helix stabilization (whether measured as the simulation drift from the initial conformation, or as the fluctuations about an average conformation) between the three different environments, with TFE/water < micelles < bilayers. Thus, although TFE seems to stabilize, to a limited extent, an intrinsic propensity of the M2GlyR peptides to α-helicity, it does not ''force'' α-helicity upon peptides or regions of peptides that have an intrinsically low helix propensity. This is consistent with a number of experimental studies, although there have also been some reports of α-helix being induced in regions that adopt a β-strand conformation in the native state of the protein (64,65). The stabilization of the α-helical conformation seems to be related to the clustering of TFE molecules around the folded peptide (66) as has been seen in previous simulation studies of peptides in TFE/water (37).

The increased stabilization of the α-helical conformation of the M2GlyR peptides by a detergent micelle and lipid bilayer environments is consistent with the two-state model of membrane protein folding (4,8). This is supported by the further stabilization of the α-helical conformation in these environments by the S22W and T19R substitutions. Tryptophan residues and basic residues at either end have been shown by a variety of methodologies, to stabilize TM helices, including structural bioinformatics (67,68), biophysical studies of synthetic peptides (69–71), and studies of biosynthetic membrane helix insertion (72).

Significantly, the trend in peptide stabilization in membrane and membrane-like environments observed in the simulation parallel experimental studies, which have demonstrated that T19R,S22W is the best channel-forming peptide of the three, in terms of induced conductivity in membranes, decreased aggregation propensity in aqueous solution, and increased aqueous solubility (see companion article). This supports the

contention that channel formation by these peptides is due to self-assembly of bundles of TM α-helices (40).

Although both micelle environments stabilize the α-helical conformation of the peptides, there do seem to be some differences between SDS and DPC micelles. Thus, SDS micelles seem to be somewhat less favorable for formation of stable M2GlyR peptide helices. In particular, e.g., the RMSD for WT is higher in SDS, and T19R,S22W forms fewer contacts to SDS than to DPC molecules. Interestingly, snapshots of the SDS micelles reveal that the headgroups seem to cluster, whereas the hydrophobic tails remain extended, with the peptide occupying the edge of the micelle (as might be anticipated for amphipathic channel-forming peptides). This is in contrast with previous (somewhat shorter) MD simulations of pure SDS micelles, which suggest the formation of stable, spherical micelles (73,74). It is of course possible that there may be some relationship, as yet unexplored, to the size (i.e., number of detergent molecules) of the micelles. However, less regular micelles have also been seen in simulations of octyl glucoside (75,76). Therefore, DPC seems to be a slightly better model of a lipid bilayer, presumably because it shares a similar headgroup with phosphatidylcholine. For example, both DPC and DMPC form substantial numbers of interactions with T19R,S22W and stabilize the α-helical conformation of the peptide. Interestingly, some experimental studies have suggested differences in behavior of peptides between SDS and DPC micelles, due to favorable interactions of the tryptophan side chains with phosphocholine headgroups (38). This is of particular interest in the context of the importance of tryptophan residues in folding and stability of membrane proteins. The role of tryptophan residues has been discussed in detail by Antoranz-Contera et al. in their recent article (77) where the bulky indole side chain of tryptophan and its ability to interact electrostatically with phosphocholine headgroups of lipids have been shown to impart membrane anchoring properties to the residue during AFM experiments to extract CWALP peptides from gel-phase DPPC and DSPC bilayers. Other examples of the role of tryptophan have been discussed by Janovjak et al. (78) with respect to the stability of the extracellular loops of bacteriorhodopsin (bR). These loops have been shown to resist unfolding and all of the tryptophan residues in bR are extracellular.

The DMPC bilayer environment seems to stabilize largely α-helical conformations for all three peptides, including WT, which is more α-helical in DMPC than in DPC. Thus, the intrinsic stability of a TM α-helix in a bilayer environment, expected for M2 on the basis of the two-state folding model, does not seem to have been lost during the addition of the NK_4-terminal extension, and has been enhanced by two C-terminal residue substitutions, both of which acted to make the peptide sequence more ''TM-like''. Thus, the placement of arginine and tryptophan at positions 19 and 22, respectively, are expected to anchor the peptide at the membrane-water interface. As mentioned above, these residues are commonly found at the ends of transmembrane segments and provide stability for the membrane spanning helices (79). Thus, it would seem that 20-ns simulations are sufficient to reveal some aspects of the relative stability of different TM helices in a bilayer environment.

It is apparent that in almost all of the environments, apart from perhaps the DPC micelle, the most stable peptide is T19R,S22W. In particular, the absence of the tryptophan, with its ''membrane-anchoring'' propensity, from the WT peptide seems to destabilize the α-helical conformation in both a bilayer and bilayer-like environments.

To investigate whether the apparent increased stability of T19R,S22W when compared to the other two peptides was a direct effect of the sequence or an artifact introduced by the model building process, we also constructed an ideal α-helical model of the WT peptide (the least stable sequence) and simulated this in TFE/water (the least helix promoting environment). Although more stable than the WT NMR model in TFE/water, this model peptide was still less stable than T19R,S22W in TFE/water. This increases our confidence in the simulations starting from an ideal α-helical model of T19R,S22W. Encouragingly, the recent structure of T19R,S22W in SDS micelles (which was not known at the time of the simulation studies) is nearly entirely α-helical, apart from the N-terminal K_4 region (G. Cook and J. Tomich, unpublished data). Simulations starting from this structure yield essentially the same results as the T19R,S22W simulations described in the current article (J. M. Johnston and M. S. P. Sansom, unpublished data).

Clearly, there are limitations to the simulations performed. Analysis of the magnitude of Cα atom mean-square fluctuations as a function of the duration of the time segment over which they are averaged (data not shown; see, e.g., (31,80) for details) indicates that none of the simulations have converged, i.e., on an $\sim$20-ns timescale there is incomplete sampling of the protein conformational space (81). However, this does not preclude comparisons between peptides and environments provided the possibility of other effects on longer timescales is retained. The advantage of simulation studies is that they provide a detailed (and dynamic) view of peptide stability and interactions that complements the information derived from spectroscopic (e.g., CD and NMR) studies.

The studies described in this article contribute to ongoing efforts to understand more fully the nature of folding and self-assembly of bundles of TM α-helices (4,9,82). For example, recent simulation studies (83) have suggested a role for side-chain mediated interhelical H-bonds in TM bundle self-assembly, in agreement with recent experimental data (11,12). However, the timescales of more complex folding and self-assembly are difficult to access by all atom simulations. Recent simulation studies of folding processes of water soluble peptides (84) suggest that more approximate simulation techniques (68) may be adopted to explore membrane protein folding in more detail (85). What is evident is

that molecular simulation studies will play an increasingly important role in unmasking some of the complexities of stability and folding of both naturally occurring and synthetic membrane protein assemblies.

We thank all of our colleagues for help and advice, especially Oliver Beckstein, Peter Bond, and Sundeep Deol. We thank Danilo Roccatano for the TFE parameters.

We thank the following agencies for funding: Medical Research Council (J.M.J. and M.S.P.S.), Biotechnology and Biological Sciences Research Council, Engineering and Physical Sciences Research Council, and the Wellcome Trust (M.S.P.S.), National Institute of General Medical Sciences grant GM43617 (J.M.T.), and US Public Health Service grant GM074096 (J.M.T.).

REFERENCES

1. Wallin, E., and G. von Heijne. 1998. Genome-wide analysis of integral membrane proteins from eubacterial, archean, and eukaryotic organisms. *Protein Sci.* 7:1029–1038.
2. Terstappen, G. C., and A. Reggiani. 2001. In silico research in drug discovery. *Trends Pharmacol. Sci.* 22:23–26.
3. White, S. H. 2004. The progress of membrane protein structure determination. *Protein Sci.* 13:1948–1949.
4. Popot, J. L., and D. M. Engelman. 2000. Helical membrane protein folding, stability, and evolution. *Annu. Rev. Biochem.* 69:881–922.
5. Chopra, A., P. L. Yeagle, J. A. Alderfer, and A. D. Albert. 2000. Solution structure of the sixth transmembrane helix of the G-protein-coupled receptor, rhodopsin. *Biochim. Biophys. Acta.* 1463:1–5.
6. MacKenzie, K. R., J. H. Prestegard, and D. M. Engelman. 1997. A transmembrane helix dimer: structure and implications. *Science.* 276: 131–133.
7. Smith, S. O., D. Song, S. Shekar, M. Groesbeek, M. Ziliox, and S. Aimoto. 2001. Structure of the transmembrane dimer interface of glycophorin A in membrane bilayers. *Biochemistry.* 40:6553–6558.
8. Popot, J. L., and D. M. Engelman. 1990. Membrane protein folding and oligomerization: the two-state model. *Biochemistry.* 29:4031–4037.
9. Engelman, D. M., Y. Chen, C. Chin, R. Curran, A. M. Dixon, A. Dupuy, A. Lee, U. Lehnert, E. Mathews, Y. Reshetnyak, A. Senes, and J. L. Popot. 2003. Membrane protein folding: beyond the two stage model. *FEBS Lett.* 555:122–125.
10. Popot, J. L. 1993. Integral membrane protein structure: transmembrane α helices as autonomous folding domains. *Curr. Opin. Struct. Biol.* 3:532–540.
11. Choma, C., H. Gratkowski, J. D. Lear, and W. F. DeGrado. 2000. Asparagine-mediated self-association of a model transmembrane helix. *Nat. Struct. Biol.* 7:161–166.
12. Zhou, F. X., H. J. Merianos, A. T. Brunger, and D. M. Engelman. 2001. Polar residues drive association of polyleucine transmembrane helices. *Proc. Natl. Acad. Sci. USA.* 98:2250–2255.
13. Sansom, M. S. P. 1991. The biophysics of peptide models of ion channels. *Prog. Biophys. Mol. Biol.* 55:139–236.
14. Sansom, M. S. P. 1993. Structure and function of channel-forming peptaibols. *Q. Rev. Biophys.* 26:365–421.
15. Schubert, U., A. V. Ferrer-Montiel, M. Oblatt-Montal, P. Henklein, K. Strebel, and M. Montal. 1996. Identification of an ion channel activity of the Vpu transmembrane domain and its involvement in the regulation of virus release from HIV-1-infected cells. *FEBS Lett.* 398:12–18.
16. Lear, J. D., Z. R. Wasserman, and W. F. DeGrado. 1988. Synthetic amphiphilic peptide models for protein ion channels. *Science.* 240: 1177–1181.
17. Oiki, S., W. Danho, V. Madison, and M. Montal. 1988. M2δ, a candidate for the structure lining the ionic channel of the nicotinic cholinergic receptor. *Proc. Natl. Acad. Sci. USA.* 85:8703–8707.
18. Montal, M. 1995. Design of molecular function: channels of communication. *Annu. Rev. Biophys. Biomol. Struct.* 24:31–57.
19. Opella, S. J., F. M. Marassi, J. J. Gesell, A. P. Valente, Y. Kim, M. Oblatt-Montal, and M. Montal. 1999. Structures of the M2 channel-lining segments from nicotinic acetylcholine and NMDA receptors by NMR spectroscopy. *Nat. Struct. Biol.* 6:374–379.
20. Law, R. J., L. R. Forrest, K. M. Ranatunga, P. La Rocca, D. P. Tieleman, and M. S. P. Sansom. 2000. Structure and dynamics of the pore-lining helix of the nicotinic receptor: MD simulations in water, lipid bilayers and transbilayer bundles. *Proteins.* 39:47–55.
21. Law, R. J., D. P. Tieleman, and M. S. P. Sansom. 2003. Pores formed by the nicotinic receptor M2δ peptide: a molecular dynamics simulation study. *Biophys. J.* 84:14–27.
22. Lester, H. A., M. I. Dibas, D. S. Dahan, J. F. Leite, and D. A. Dougherty. 2004. Cys-loop receptors: new twists and turns. *Trends Neurosci.* 27:329–336.
23. Ma, D., Z. Liu, L. Li, P. Tang, and Y. Xu. 2005. Structure and dynamics of the second and third transmembrane domain of human glycine receptor. *Biochemistry.* 44:8790–8800.
24. Unwin, N. 2005. Refined structure of the nicotinic acetylcholine receptor at 4 Å resolution. *J. Mol. Biol.* 346:967–989.
25. Reddy, G. L., T. Iwamoto, J. M. Tomich, and M. Montal. 1993. Synthetic peptides and four-helix bundle proteins as model systems for the pore-forming structure of channel proteins. II. Transmembrane segment M2 of the brain glycine receptor is a plausible candidate for the pore-lining structure. *J. Biol. Chem.* 268:14608–14615.
26. Cook, G. A., O. Prakash, K. Zhang, L. P. Shank, W. A. Takeguchi, A. Robbins, Y. X. Gong, T. Iwamoto, B. D. Schultz, and J. M. Tomich. 2004. Activity and structural comparisons of solution associating and monomeric channel-forming peptides derived from the glycine receptor M2 segment. *Biophys. J.* 86:1424–1435.
27. Wallace, D. P., J. M. Tomich, T. Iwamoto, K. Henderson, J. J. Grantham, and L. P. Sullivan. 1997. A synthetic peptide derived from glycine-gated Cl^- channel induces transepithelial Cl^- and fluid secretion. *Am. J. Physiol.* 272:C1672–C1679.
28. Petrache, H. I., A. Grossfield, K. R. MacKenzie, D. M. Engelman, and T. B. Woolf. 2000. Modulation of glycophorin A transmembrane helix interactions by lipid bilayers: molecular dynamics calculations. *J. Mol. Biol.* 302:727–746.
29. Ash, W. L., M. R. Zlomislic, E. O. Oloo, and D. P. Tieleman. 2004. Computer simulations of membrane proteins. *Biochim. Biophys. Acta.* 1666:158–189.
30. Sengupta, D., L. Meinhold, D. Langosch, G. M. Ullmann, and J. C. Smith. 2005. Understanding the energetics of helical peptide orientation in membranes. *Proteins.* 58:913–922.
31. Bond, P. J., and M. S. P. Sansom. 2003. Membrane protein dynamics vs. environment: simulations of OmpA in a micelle and in a bilayer. *J. Mol. Biol.* 329:1035–1053.
32. Bond, P. J., J. M. Cuthbertson, S. D. Deol, and M. S. P. Sansom. 2004. MD simulations of spontaneous membrane protein/detergent micelle formation. *J. Am. Chem. Soc.* 126:15948–15949.
33. Braun, R., D. M. Engelman, and K. Schulten. 2004. Molecular dynamics simulations of micelle formation around dimeric glycophorin A transmembrane helices. *Biophys. J.* 87:754–763.
34. Saiz, L., and M. L. Klein. 2002. Structure of the pore region of the nicotinic acetylcholine receptor ion channel: a molecular dynamics simulation study. *Biophys. J.* 82:560a. (Abstr.).
35. Saiz, L., S. Bandyopadhyay, and M. L. Klein. 2004. Effect of the pore region of a transmembrane ion channel on the physical properties of a simple membrane. *J. Phys. Chem. B.* 108:2608–2613.
36. Kessel, A., D. Shental-Bechor, T. Haliloglu, and N. Ben-Tal. 2003. Interactions of hydrophobic peptides with lipid bilayers: Monte Carlo simulations with M2 delta. *Biophys. J.* 85:3431–3444.

37. Roccatano, D., G. Colombo, M. Fioroni, and A. E. Mark. 2002. Mechanism by which 2,2,2-trifluoroethanol/water mixtures stabilize secondary-structure formation in peptides: a molecular dynamics study. *Proc. Natl. Acad. Sci. USA*. 99:12179–12184.

38. Neidigh, J. W., and N. H. Andersen. 2002. Peptide conformational changes induced by tryptophan-phosphocholine interactions in a micelle. *Biopolymers*. 65:354–361.

39. Tang, P., P. K. Mandal, and Y. Xu. 2002. NMR structures of the second transmembrane domain of the human glycine receptor alpha(1) subunit: model of pore architecture and channel gating. *Biophys. J.* 83:252–262.

40. Broughman, J. R., L. P. Shank, W. Takeguchi, T. Iwamoto, K. E. Mitchell, B. D. Schultz, and J. M. Tomich. 2002. Distinct structural elements that direct solution aggregation and membrane assembly in the channel forming peptide M2GlyR. *Biochemistry*. 41:7350–7358.

41. Kerr, I. D., R. Sankararamakrishnan, O. S. Smart, and M. S. P. Sansom. 1994. Parallel helix bundles and ion channels: molecular modelling via simulated annealing and restrained molecular dynamics. *Biophys. J.* 67:1501–1515.

42. Kerr, I. D., and M. S. P. Sansom. 1993. Hydrophilic surface maps of α-helical channel-forming peptides. *Eur. Biophys. J.* 22:269–277.

43. Lindahl, E., B. Hess, and D. van der Spoel. 2001. GROMACS 3.0: a package for molecular simulation and trajectory analysis. *J. Mol. Model.* [Online]. 7:306–317.

44. Berendsen, H. J. C., J. P. M. Postma, W. F. van Gunsteren, and J. Hermans. 1981. Intermolecular Forces. Reidel, Dordrecht, The Netherlands.

45. van der Spoel, D., P. J. van Maaren, and H. J. C. Berendsen. 1998. A systematic study of water models for molecular simulations. *J. Chem. Phys.* 108:10220–10230.

46. Berendsen, H. J. C., J. P. M. Postma, W. F. van Gunsteren, A. DiNola, and J. R. Haak. 1984. Molecular dynamics with coupling to an external bath. *J. Chem. Phys.* 81:3684–3690.

47. Nose, S. 1984. A molecular dynamics method for simulations in the canonical ensemble. *Mol. Phys.* 52:255–268.

48. Hoover, W. G. 1985. Canonical dynamics: equilibrium phase-space distributions. *Phys. Rev.* A31:1695–1697.

49. Parrinello, M., and A. Rahman. 1981. Polymorphic transitions in single-crystals: a new molecular-dynamics method. *J. Appl. Phys.* 52: 7182–7190.

50. Darden, T., D. York, and L. Pedersen. 1993. Particle mesh Ewald: an N.log(N) method for Ewald sums in large systems. *J. Chem. Phys.* 98:10089–10092.

51. Hess, B., H. Bekker, H. J. C. Berendsen, and J. G. E. M. Fraaije. 1997. LINCS: a linear constraint solver for molecular simulations. *J. Comput. Chem.* 18:1463–1472.

52. Fioroni, M., K. Burger, A. E. Mark, and D. Roccatano. 2000. A new 2,2,2-trifluoroethanol model for molecular dynamics simulations. *J. Phys. Chem. B.* 104:12347–12354.

53. Fioroni, M., M. D. Diaz, K. Burger, and S. Berger. 2002. Solvation phenomena of a tetrapeptide in water/trifluoroethanol and water/ethanol mixtures: a diffusion NMR, intermolecular NOE, and molecular dynamics study. *J. Am. Chem. Soc.* 124:7737–7744.

54. van Aalten, D. M., R. Bywater, J. B. Findlay, M. Hendlich, R. W. Hooft, and G. Vriend. 1996. PRODRG, a program for generating molecular topologies and unique molecular descriptors from coordinates of small molecules. *J. Comput. Aided Mol. Des.* 10:255–262.

55. Faraldo-Gómez, J. D., G. R. Smith, and M. S. P. Sansom. 2002. Setup and optimisation of membrane protein simulations. *Eur. Biophys. J.* 31:217–227.

56. Kabsch, W., and C. Sander. 1983. Dictionary of protein secondary structure: pattern-recognition of hydrogen-bonded and geometrical features. *Biopolymers*. 22:2577–2637.

57. Laskowski, R. A., M. W. Macarthur, D. S. Moss, and J. M. Thornton. 1993. Procheck: a program to check the stereochemical quality of protein structures. *J. Appl. Crystallogr.* 26:283–291.

58. Humphrey, W., A. Dalke, and K. Schulten. 1996. VMD: visual molecular dynamics. *J. Mol. Graph.* 14:33–38.

59. Sayle, R. A., and E. J. Milner-White. 1995. RasMol: biomolecular graphics for all. *Trends Biochem. Sci.* 20:374–376.

60. Schiffer, M., C. H. Chang, and F. J. Stevens. 1992. The functions of tryptophan residues in membrane proteins. *Protein Eng.* 5:213–214.

61. Yau, W. M., W. C. Wimley, K. Gawrisch, and S. H. White. 1998. The preference of tryptophan for membrane interfaces. *Biochemistry*. 37: 14713–14718.

62. de Planque, M. R., B. B. Bonev, J. A. Demmers, D. V. Greathouse, R. E. Koeppe, F. Separovic, A. Watts, and J. A. Killian. 2003. Interfacial anchor properties of tryptophan residues in transmembrane peptides can dominate over hydrophobic matching effects in peptide-lipid interactions. *Biochemistry*. 42:5341–5348.

63. Deol, S. S., P. J. Bond, C. Domene, and M. S. P. Sansom. 2004. Lipid-protein interactions of integral membrane proteins: a comparative simulation study. *Biophys. J.* 87:3737–3749.

64. Nelson, J. W., and N. R. Kallenbach. 1986. Stabilization of the ribonuclease S-peptide alpha-helix by trifluoroethanol. *Proteins*. 1:211–217.

65. Shiraki, K., K. Nishikawa, and Y. Goto. 1995. Trifluoroethanol-induced stabilization of the alpha-helical structure of beta-lactoglobulin: implication for non-hierarchical protein folding. *J. Mol. Biol.* 245:180–194.

66. Hong, D. P., M. Hoshino, R. Kuboi, and Y. Goto. 1999. Clustering of fluorine-substituted alcohols as a factor responsible for their marked effects on proteins and peptides. *J. Am. Chem. Soc.* 121:8427–8433.

67. Ulmschneider, M. B., and M. S. P. Sansom. 2001. Amino acid distributions in integral membrane protein structures. *Biochim. Biophys. Acta*. 1512:1–14.

68. Ulmschneider, M. B., M. S. P. Sansom, and A. Di Nola. 2005. Properties of integral membrane protein structures: derivation of an implicit membrane potential. *Proteins*. 59:252–265.

69. de Planque, M. R. R., J. A. W. Kruijtzer, R. M. J. Liskamp, D. Marsh, D. V. Greathouse, R. E. Koeppe, B. de Kruijff, and J. A. Killian. 1999. Different membrane anchoring positions of tryptophan and lysine in synthetic transmembrane alpha-helical peptides. *J. Biol. Chem.* 274: 20839–20846.

70. de Planque, M. R. R., and J. A. Killian. 2003. Protein-lipid interactions studied with designed transmembrane peptides: role of hydrophobic matching and interfacial anchoring. *Mol. Membr. Biol.* 20:271–284.

71. Killian, J. A. 2003. Synthetic peptides as models for intrinsic membrane proteins. *FEBS Lett.* 555:134–138.

72. Hessa, T., H. Kim, K. Bihlmaier, C. Lundin, J. Boekel, H. Andersson, I. Nilsson, S. H. White, and G. von Heijne. 2005. Recognition of transmembrane helices by the endoplasmic reticulum translocon. *Nature*. 433:377–381.

73. Bruce, C. D., S. Senapati, M. L. Berkowitz, L. Perera, and M. D. E. Forbes. 2002. Molecular dynamics simulations of sodium dodecyl sulfate micelle in water: the behavior of water. *J. Phys. Chem. B.* 106:10902–10907.

74. Bruce, C. D., M. L. Berkowitz, L. Perera, and M. D. E. Forbes. 2002. Molecular dynamics simulation of sodium dodecyl sulfate micelle in water: micellar structural characteristics and counterion distribution. *J. Phys. Chem. B*. 106:3788–3793.

75. Bogusz, S., R. M. Venable, and R. W. Pastor. 2000. Molecular dynamics simulations of octyl glucoside micelles: structural properties. *J. Phys. Chem. B*. 104:5462–5470.

76. Bogusz, S., R. M. Venable, and R. W. Pastor. 2001. Molecular dynamics simulations of octyl glucoside micelles: dynamic properties. *J. Phys. Chem. B*. 105:8312–8321.

77. Antoranz-Contera, S., V. Lemaitre, M. R. de Planque, A. Watts, and J. F. Ryan. 2005. Unfolding and extraction of a transmembrane α-helical peptide: dynamic force spectroscopy and molecular dynamics simulations. *Biophys. J.* 89:3129–3140.

78. Janovjak, H., J. Struckmeier, M. Hubain, A. Kedrov, M. Kessler, and D. J. Muller. 2004. Probing the energy landscape of the membrane protein bacteriorhodopsin. *Structure*. 12:871–879.

79. Killian, J. A., and G. von Heijne. 2000. How proteins adapt to a membrane-water interface. *Trends Biochem. Sci.* 25:429–434.

80. Faraldo-Gómez, J. D., G. R. Smith, and M. S. P. Sansom. 2003. Molecular dynamics simulations of the bacterial outer membrane protein FhuA: a comparative study of the ferrichrome-free and bound states. *Biophys. J.* 85:1–15.

81. Faraldo-Gómez, J. D., L. R. Forrest, M. Baaden, P. J. Bond, C. Domene, G. Patargias, J. Cuthbertson, and M. S. P. Sansom. 2004. Conformational sampling and dynamics of membrane proteins from 10-nanosecond computer simulations. *Proteins*. 57:783–791.

82. Curran, A. R., and D. Engelman. 2003. Sequence motifs, polar interactions and conformational changes in membrane proteins. *Curr. Opin. Struct. Biol.* 13:412–417.

83. Stockner, T., W. L. Ash, J. L. MacCallum, and D. P. Tieleman. 2004. Direct simulation of transmembrane helix association: role of asparagines. *Biophys. J.* 87:1650–1656.

84. Chowdhury, S., M. C. Lee, G. Xiong, and Y. Duan. 2003. *Ab initio* folding simulation of the Trp-cage mini-protein approaches NMR resolution. *J. Mol. Biol.* 327:711–717.

85. Im, W., and C. L. Brooks. 2005. Interfacial folding and membrane insertion of designed peptides studied by molecular dynamics simulations. *Proc. Natl. Acad. Sci. USA*. 102:6771–6776.